




## Research Article

# Modelling and Simulation of the Effect of Irradiance Related Temperature on Microalgae Cell Growth in an Outdoor Culture for a Horizontal Loop Tubular Photobioreactor

Md. Kamrul Hasan Chowdury<sup>1</sup>, Md. Rashedul Islam<sup>1,2</sup>, Nurun Nahar<sup>1\*</sup>, Mohammad Iftexhar Monir<sup>3</sup>, Ujjwal Kumar Deb<sup>1</sup>

<sup>1</sup>Department of Mathematics, Chittagong University of Engineering & Technology, Chattogram, Bangladesh

<sup>2</sup>Department of Computer Science and Engineering, International Islamic University Chittagong, Chattogram, Bangladesh

<sup>3</sup>Department of Mathematics, Premier University, Chattogram, Bangladesh

E-mail: naharcuet@gmail.com

**Received:** 11 June 2023; **Revised:** 7 September 2023; **Accepted:** 28 September 2023

**Abstract:** Microalgae growth is influenced by numerous culture parameters, and temperature is considered one of the vital growth factors among them. In this study, a computational growth model related for a microalgae cell growth to irradiance related temperature for an outdoor operated Horizontal Loop Tubular Photobioreactor (HLTP) is developed. The effects of direct and diffuse solar radiation on the Photobioreactor (PBR) temperature are considered in this model. An HLTP measuring length 20.5 m and radius 0.025 m has been assumed for the simulation model. The simulation is carried out on a specific date where the sunlight is considered available. Thus, the meteorological data associated with a geographic location has been collected for the simulation while the species of microalgae is *Chlorella vulgaris*. The present model is simulated by COMSOL Multiphysics version 4.2 and a temperature fluctuation between 24.85 °C and 38.45 °C is observed throughout the PBR domain. The velocity profile of the suspension flow is also analysed in this study. The present study suggests that necessary measures are needed to control the temperature to reduce cell damage.

**Keywords:** microalgae, biofuel, photobioreactor, solar irradiance, temperature

**MSC:** 76-10

## 1. Introduction

Global warming has become one of the most pressing issues of the world over the last few decades. The consequence of global warming can be experienced from climate change. Due to the advent of industrialization and motorization, the use of fossil fuels has been increasing extensively releasing huge amount of greenhouse gases resulting global warming and climate change [1]. Moreover, these fossil fuels are being continuously exhausted due to widespread use in transportation sector and industries. In addition, fossil fuels are non-renewable. If we are unable to manage proper and economical alternative for fossil fuels before their depletion, the future scenario of fuel industry would be a catastrophe. Thus, an efficient utilization of the available renewable natural resources is necessary to meet this global energy demand. Biofuels could be a promising alternative because they are renewable and eco-friendly.

---

Copyright ©2025 Nurun Nahar, et al.  
DOI: <https://doi.org/10.37256/cm.6120253205>  
This is an open-access article distributed under a CC BY license  
(Creative Commons Attribution 4.0 International License)  
<https://creativecommons.org/licenses/by/4.0/>

There are many feedstocks available for biofuel production, such as Soybeans, Rapeseeds, Sunflower, Castor, Palm oil, microalgae etc. Microalgae are considered one of the best feedstocks among them [2].

There are mainly two categories of microalgae culture systems: the open raceway pond system and the closed PBR method. The open systems are strongly weather dependent. Moreover, in the open system, microbial contamination risk, CO<sub>2</sub> loss and land requirement is also higher compared to closed systems. Yet, construction cost is much lower in the open system than that of closed systems [3, 4]. Due to the limited control of cultivation conditions and contamination risk, the open systems are constrained to a relatively small number of microalgae species. Alternatively, since closed PBRs support a controlled environment, potentially free of contaminants, much wider selection of strains can be produced. Therefore, analysing pros and cons in both the systems, the closed PBR method is chosen as the best culture system for microalgae production.

In phototrophic microalgae culture system, the major requirements that must be fulfilled are the supply of light and nutrients (Carbon, Nitrogen, Phosphorous, etc.), the maintenance of adequate culture conditions, pH, Temperature, etc. and mixing to avoid gradients of these parameters that lowers the yield of biological system [5, 6]. As temperature plays a key role in microalgae cultivation process, the controlling of temperature is necessary for the better performance of a PBR [7]. Thus, to control the broth temperature, it is necessary to develop a temperature model that is affected by the environmental parameters. The optimal temperature for microalgae growth ranges between 20 °C and 35 °C, some mesophilic species can tolerate up to 40 °C though [8]. The yield of strain gets reduced below the optimal temperature, but overheating of the cultures is considered as critical because it damages microalgae cells [9]. Therefore, seasonal variations have significant effects on microalgae cultivation as it leads to the temperature variations during the day/night cycle. Temperature control is not required for small-scale reactors because the air surrounding system is cold enough to maintain the favourable ambience. However, the solar radiation is high in the outdoor large-scale reactors, and thus, it is imperative to use additional heat control systems to avoid overheating [10, 11]. Several researchers [12-16] have investigated the temperature effect on the biomass and lipid yield of microalgae. By studying various microalgae strains, Gonçalves et al. [12] found that the optimum temperature for the growth of *C. vulgaris* is 25 °C. Studies on microalgae growth related to the light irradiance have been studied earlier, and the previous researchers [17-22] found a good response in growth with respect to the light irradiance.

To simulate hydrodynamics, heat and mass transfer, computational fluid dynamics (CFD) plays a significant role when resources and time spent becomes impediments for real experimental set-up [23]. CFD simulation of temperature effect on microalgae growth for local solar irradiance considering direct solar radiation is carried out by many researchers [24, 25]. The present study aims to develop a mathematical model for an HLTP considering both direct and diffuse solar radiation and then simulate the probable impacts on the microalgae growth for the geographical location of Chittagong University of Engineering and Technology (CUET), Chattogram, Bangladesh.

## 2. Research methodology

### 2.1 Mathematical modelling

It is necessary to study feasibility analysis of a model before its implementation which is sometimes very expensive and time consuming. In these circumstances, simulation plays a vital role to create an environment which gives almost same results that can be experienced from the real experiment. It is known that the temperature works as a controlling parameter for microalgae growth. Thus, the effect of direct and diffuse solar radiation that heats up the PBR directly with varying solar position is considered for our simulation. Firstly, a mathematical model of temperature change in outdoor operated HLTP is developed. In this model, the algal suspension is considered as an incompressible viscous single-phase Newtonian fluid and the flow problem is single phase laminar flow in the creeping state. So, the governing equations are the equation of continuity and the Navier-Stokes equations coupled with heat transfer equation for non-isothermal laminar flow. For the simplicity of the model, in the energy balance equation, we consider the net radiative heat as the sum of direct and diffuse solar radiation. The relevant meteorological data are considered for the geographic location of CUET.

## 2.2 Governing equations

We considered the algae suspension and flow dynamics as Newtonian incompressible fluid and laminar flow respectively. Therefore, the flow phenomena satisfy continuity equation and Navier-Stokes equation as given below:

$$\frac{\partial \rho}{\partial t} + \nabla \cdot (\rho \mathbf{u}) = 0 \quad (1)$$

$$\rho \frac{\partial \mathbf{u}}{\partial t} = \nabla \cdot \left[ -p \mathbf{I} + \mu \left( \nabla \mathbf{u} + (\nabla \mathbf{u})^T \right) - \frac{2}{3} \mu (\nabla \cdot \mathbf{u}) \mathbf{I} \right] + \mathbf{F} \quad (2)$$

where,  $\rho$  is the density ( $\text{kgm}^{-3}$ ) of the reactor medium,  $\mathbf{u}$  is the flow velocity ( $\text{ms}^{-1}$ ),  $\mu$  is the dynamic viscosity ( $\text{kgm}^{-1}\text{s}^{-1}$ ),  $\mathbf{I}$  stands for identity matrix, and  $\mathbf{F}$  represents the body force (N).

The heat transfer equation for a non-isothermal laminar flow is

$$\rho C_p \left( \frac{\partial T}{\partial t} + \mathbf{u} \cdot \nabla T \right) = \nabla \cdot (k \nabla T) \quad (3)$$

where,  $C_p$  represents the specific heat capacity ( $\text{Jkg}^{-1}\text{K}^{-1}$ ) of the suspension,  $T$  is the reactor broth temperature (K) and  $k$  is the thermal conductivity ( $\text{Wm}^{-1}\text{K}^{-1}$ ).

The dynamic viscosity  $\mu$  in (2) is given by

$$\mu = \mu_0 (1 + \varepsilon C(t)) \quad (4)$$

where,  $\varepsilon$  stands for Einstein's coefficient [26],  $\mu_0$  is the water viscosity ( $\text{kgm}^{-1}\text{s}^{-1}$ ) and  $C(t)$  is the cell concentration at any time  $t$  (g/L). Based on the experimental data obtained by Hon-nami and Kunito [27], the cell concentration  $C(t)$  in (4) depends on the microalgae growth rate ( $\mu_m$ ) which can be expressed by the following logistic function.

$$C(t) = C_0 + \frac{a}{1 + b \exp(-\mu_m t)} \quad (5)$$

where,  $C_0$  represents the initial concentration of the suspension, and  $a$  and  $b$  are constants.

One dimensional energy balance equation can be written as follows [28]

$$\rho C_p \frac{dT}{dt} = Q_{\text{radiation}(total)} \quad (6)$$

where,  $Q_{\text{radiation}(total)}$  represents the total solar radiation (W).

Total solar radiation to the reactor system is the sum of the direct solar radiation ( $Q_{\text{rad}, D}$ ) (W) and the diffuse solar radiation ( $Q_{\text{rad}, d}$ ) (W) [29], i.e.

$$Q_{\text{radiation}(total)} = Q_{\text{rad}, D} + Q_{\text{rad}, d} \quad (7)$$

We can estimate the direct solar radiation ( $Q_{\text{rad}, D}$ ) (W) on the surface of the reactor from following equation [28]

$$Q_{rad, D} = \tau \varepsilon_r H_D A_r f_A f(t) \cos \theta \quad (8)$$

where,  $\tau$  represents the transmissivity of the reactor,  $\varepsilon_r$  is the emissivity of the reactor medium,  $H_D$  is the intensity of the direct solar radiation ( $\text{Wm}^{-2}$ ) reaching to the ground vertically,  $\theta$  is the angle of incidence (rad),  $A_r$  is the outer surface area ( $\text{m}^2$ ) of the reactor that is exposed to atmosphere,  $f_A$  is the form factor between the reactor surface and the atmosphere, and  $f(t)$  is the shading function.

The shading function,  $f(t)$  is equal to 1 when the reactor is exposed to the sun, else equal to zero [29]. The form factor ( $f_A$ ) for the reactor is 0.5, and therefore, equation (8) reduces to

$$Q_{rad, D} = \tau \varepsilon_r H_D \pi R L \cos \theta \quad (9)$$

where,  $R$  is the outer radius (m) and  $L$  is the length (m) of the reactor tube.

In general, solar radiation varies with the angular position ( $\theta$ ) of the incident sunlight. This angular position depends on five parameters, namely: declination ( $\delta$ ), geographic latitude ( $\phi$ ), surface slope ( $\beta$ ), surface azimuth angle ( $\tau$ ) and the hour angle ( $\omega$ ). These five parameters are related by the following equation [30].

$$\begin{aligned} \cos \theta = & \sin \delta \sin \phi \cos \beta - \sin \delta \cos \phi \sin \beta \cos \tau \\ & + \cos \delta \cos \phi \cos \beta \cos \omega + \cos \delta \sin \beta \sin \tau \sin \omega \end{aligned} \quad (10)$$

PBR placed in horizontal position has an exposure to larger illumination area than any other position with respect to the variation in solar hour [31]. Hence, the surface slope ( $\beta$ ) is set to zero degree that yields the equation (10) in its simplest form,

$$\cos \theta = \sin \delta \sin \phi + \cos \delta \cos \phi \cos \omega \quad (11)$$

The solar declination angle ( $\delta$ ) which is a function of the day of the year ( $N$ ) can be found from following equation [30].

$$\delta = 23.35 \left( \frac{\pi}{180} \right) \sin \left[ \frac{2\pi}{365} (284 + N) \right] \quad (12)$$

The hour angle ( $\omega$ ) is a function of the solar hour ( $sh$ ) which can be evaluated from following equation. It is typically negative before noon and positive in the afternoon [30].

$$\omega = 15(sh - 12) \quad (13)$$

Diffuse radiation ( $Q_{rad, d}$ ) is the radiation resulting from the scattering of solar beams by molecules or suspensions in the atmosphere. It is not dependent on the angle of incidence ( $\theta$ ) and is evenly radiated in all directions. Applying the form factor theory, it can be expressed as [28].

$$Q_{rad, d} = \tau \varepsilon_r H_d \pi R L \quad (14)$$

where,  $H_d$  represents the intensity of the diffuse solar radiation ( $\text{W/m}^2$ ).

The direct ( $H_D$ ) and diffuse ( $H_d$ ) solar radiation can be represented as functions of the total radiation reaching the horizontal surface ( $H$ ) and the fraction of diffuse radiation impacting the ground ( $K_d$ ) [28].

$$H_d = HK_d \quad (15)$$

$$H_D = (1 - K_d)H \quad (16)$$

The value of  $K_d$  varies from 0.33 to 0.5 for low altitude areas to high altitude areas [32].

Almorox et al. [32] established a relationship between the total solar radiation ( $H$ ) and the global solar radiation ( $H_0$ ) as follows

$$\frac{H}{H_0} = a_1 \exp \left[ b_1 \left( \frac{S}{S_0} \right) \right] \quad (17)$$

where,  $a_1$  and  $b_1$  are regression coefficients that depend on the specific geographical location. Values of these coefficients are collected from the data of Sarkar [33] for Chattogram.

Global solar radiation ( $H_0$ ) can be written as follows [29].

$$H_0 = \frac{24 \times 3600}{\pi} G_{sc} \left[ 1 + 0.033 \cos \left( \frac{360N}{365} \right) \right] \left( \cos \delta \cos \phi \cos \omega + \frac{\pi}{180} \omega \sin \delta \sin \phi \right) \quad (18)$$

The day length  $S_0$  can be evaluated from the following equation [30].

$$S_0 = \frac{2}{15} \omega \quad (19)$$

One can estimate sunshine duration from cloud fraction of Bangladesh from the following linear relationship between the cloud fraction  $C$  and  $1 - \frac{S}{S_0}$  [33].

$$C = 1 - \frac{S}{S_0} \quad (20)$$

The transmittance property of the PBR helps keeping the broth temperature within the optimum range. Transmitted radiation can be written as the product of transmittance of the reactor and the transmittance of the microalgae [30] such as

$$\tau = \tau_T \tau_A \quad (21)$$

where,  $\tau_T$  represents the reactor transmittance which can be determined from following equation [30].

$$\tau_T = 0.5 \left( \frac{1 - R_{para}}{1 + R_{para}} + \frac{1 - R_{perp}}{1 + R_{perp}} \right) \quad (22)$$

where,  $R_{para}$  and  $R_{perp}$  stands for parallel and perpendicular reflection from the tube respectively and can be calculated from following equations [30].

$$R_{para} = \frac{\tan^2(\theta_2 - \theta)}{\tan^2(\theta_2 + \theta)} \quad (23)$$

$$R_{perp} = \frac{\sin^2(\theta_2 - \theta)}{\sin^2(\theta_2 + \theta)} \quad (24)$$

where,  $\theta_2$  represents the angle after refraction from the transparent tube surface, which is a function of the angle of incidence  $\theta$  of sunlight and the refraction indices of air and the reactor [30].

$$\sin \theta_2 = \left( \frac{IR_{air}}{IR_{reactor}} \right) \sin \theta \quad (25)$$

The transmittance of the algae cells can be calculated from Bouguer's law [30].

$$\tau_A = \exp\left(-K_a \frac{PL}{\cos \theta_2}\right) \quad (26)$$

where,  $K_a$  is the extinction coefficient of the microalgae cells varies from species to species. Thus, the value of  $K_a$  is taken for *C. vulgaris*,  $PL$  is the total path length which is assumed to be the 60% of the total tube diameter [34].

### 2.3 Computational domain and mesh design

Generally, an HLTP with multiple U-loops, as shown in Figure 1, is considered for mass production of microalgae.

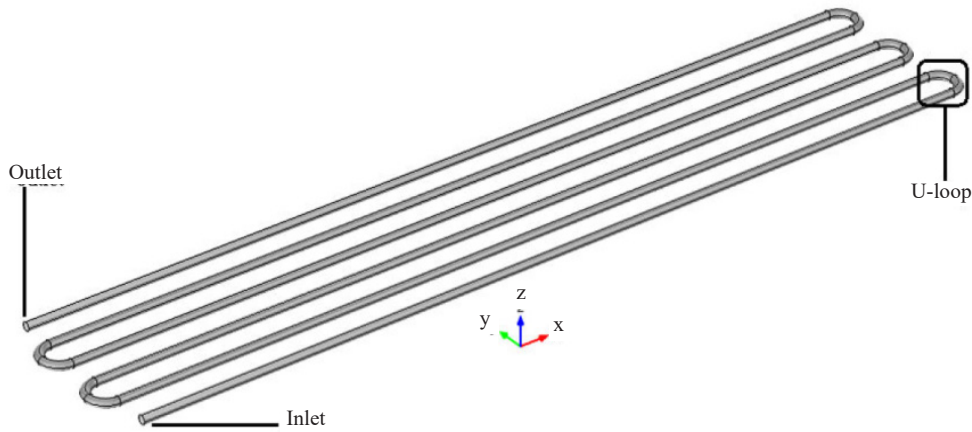


**Figure 1.** Computational domain for a microalgae flow in an HLTP with U-loop marked by a square, inlet and outlet surfaces

However, in the present study, we have proposed an HLTP with a single U-loop as the domain, where each straight portion is 10 m long and the U-loop is roughly 0.5 m. The radius, surface area and volume of the PBR are 0.025 m, 3.136 m<sup>2</sup> and 0.03679 m<sup>3</sup> respectively as shown in Figure 2. A coarse mesh design is developed with 102,822 elements for the simulation. There are 74,662 Tetrahedral elements, 28,160 Prism elements, 28,320 Triangular elements, 48 Quadrilateral elements, 4,732 Edge elements, 20 Vertex elements in the mesh. In Figure 3, the mesh designs for (a) the U-loop and (b)

the inlet are shown respectively.

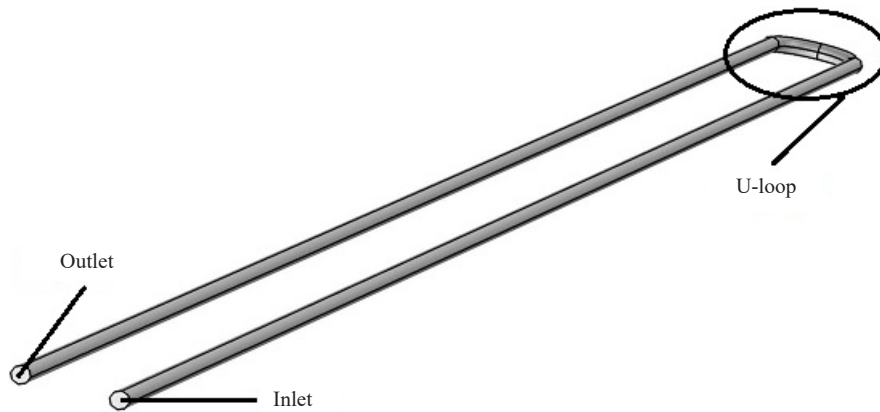


**Figure 2.** A computational domain of the HLTP showing inlet, outlet and U-loop

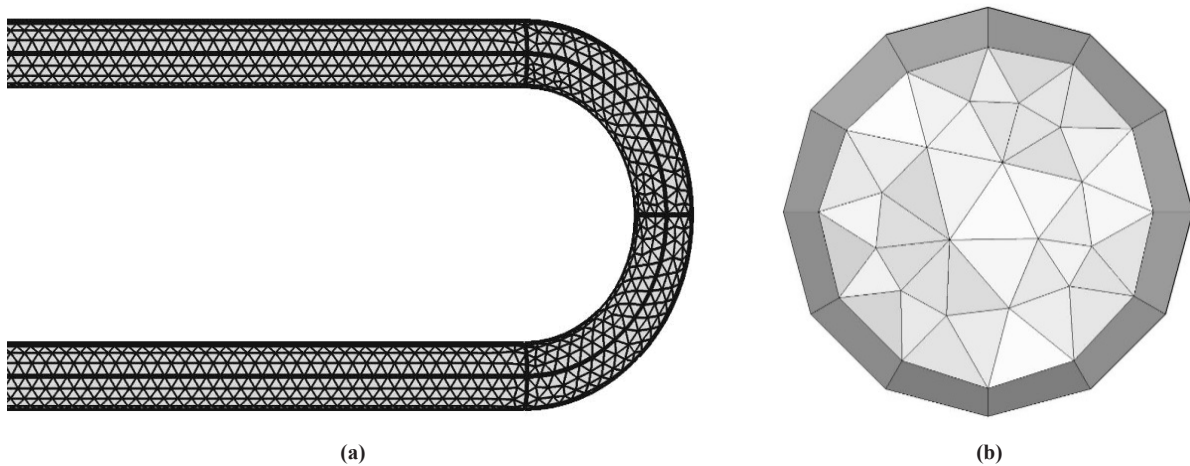


**Figure 3.** The mesh design: (a) longitudinal view and (b) cross-sectional view

## 2.4 Initial and boundary conditions

The microalgae suspension flow is assumed to be uniform in this simulation. The initial and boundary conditions are as follows:

At the inlet: initial velocity  $\mathbf{u} = (0.5, 0, 0)$ .

At the wall: No slip condition is applied, i.e.  $\mathbf{u} = 0$ .

At the outlet: normal stress is zero, i.e.

$$\left[ -p\mathbf{I} + \mu \left( \nabla \mathbf{u} + (\nabla \mathbf{u})^T \right) - \frac{2}{3} \mu (\nabla \cdot \mathbf{u}) \mathbf{I} \right] \mathbf{n} = \mathbf{0}$$

Heat flux is equal to the total radiation per unit area, i.e.

$$-\mathbf{n} \cdot (-k\nabla T) = \frac{Q_{radiation(total)}}{A}$$

Initial Temperature:  $T = 298 \text{ K}$ .

The simulation was carried out on the 16<sup>th</sup> March, the 7<sup>th</sup> day of culture, from 8:50 AM to 11:50 AM with 10 minutes interval at the geographical location of CUET.

## 2.5 Model inputs and simulation parameters

The model inputs and the simulation parameters are given in the Table 1 and in the Table 2 respectively.

**Table 1.** Model Inputs

Name	Value	Description
$p$	1 Pa	Absolute pressure
$\kappa$	0.6096 W/(m·K)	Thermal conductivity
$\rho$	1,020 kg/m <sup>3</sup>	Density
$C_p$	4,178 J/(kg·K)	Heat capacity
$\gamma$	1	Ratio of specific heats

**Table 2.** Parameters used for simulation

Name	Value	Description
$R$	0.025 m	Radius of the reactor
$V$	0.03679 m <sup>3</sup>	Volume of the reactor
$A$	3.136 m <sup>2</sup>	Area of the reactor
$IR_{air}$	1	Refraction index of air
$IR_{tube}$	1.49	Refraction index of acrylic tube
$\phi$	22.46 <sup>0</sup>	Latitude of CUET
$N$	75	Day of the year
$\varepsilon$	0.94	Emissivity of the reactor
$K_a$	36.9 m <sup>-1</sup>	Extinction coefficient of <i>C. vulgaris</i>
$\mu_{max}$	0.0631 h <sup>-1</sup>	Maximum growth rate of microalgae
$a$	1	Constant value



Table 2. (cont.)

Name	Value	Description
$b$	200	Constant value
$C_0$	0.55 g/L	Initial concentration of microalgae
$\mu_0$	0.001 Pa.s	Water viscosity
$G_{on}$	1367 W/m <sup>2</sup>	Solar constant
$PL$	0.03 m	Path length of the radiation
$K_d$	0.33	Fraction of the diffused reaction
$S$	8.1 h	Bright sunshine hour in the month of march

### 3. Simulation results

The aim of this simulation was to observe the change of temperature in the PBR and consequently its effect on the growth of microalgae for a specific geometry, species and location. All the parameters assumed here are for the outdoor culture condition, and for simulation, COMSOL Multiphysics 4.2 is used.

The velocity profile at the horizontal cross-section ( $z = 0$  plane) passing through the centre of the tube is shown in Figure 4. The legend of this figure is clearly displaying that the velocity is higher in the middle of the tube compared to that of the wall, which gives a parabolic shape of the profile.

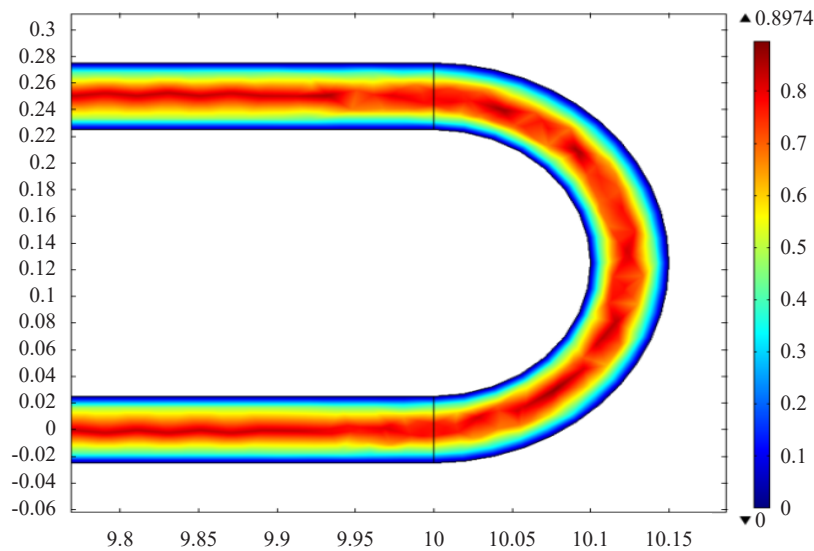
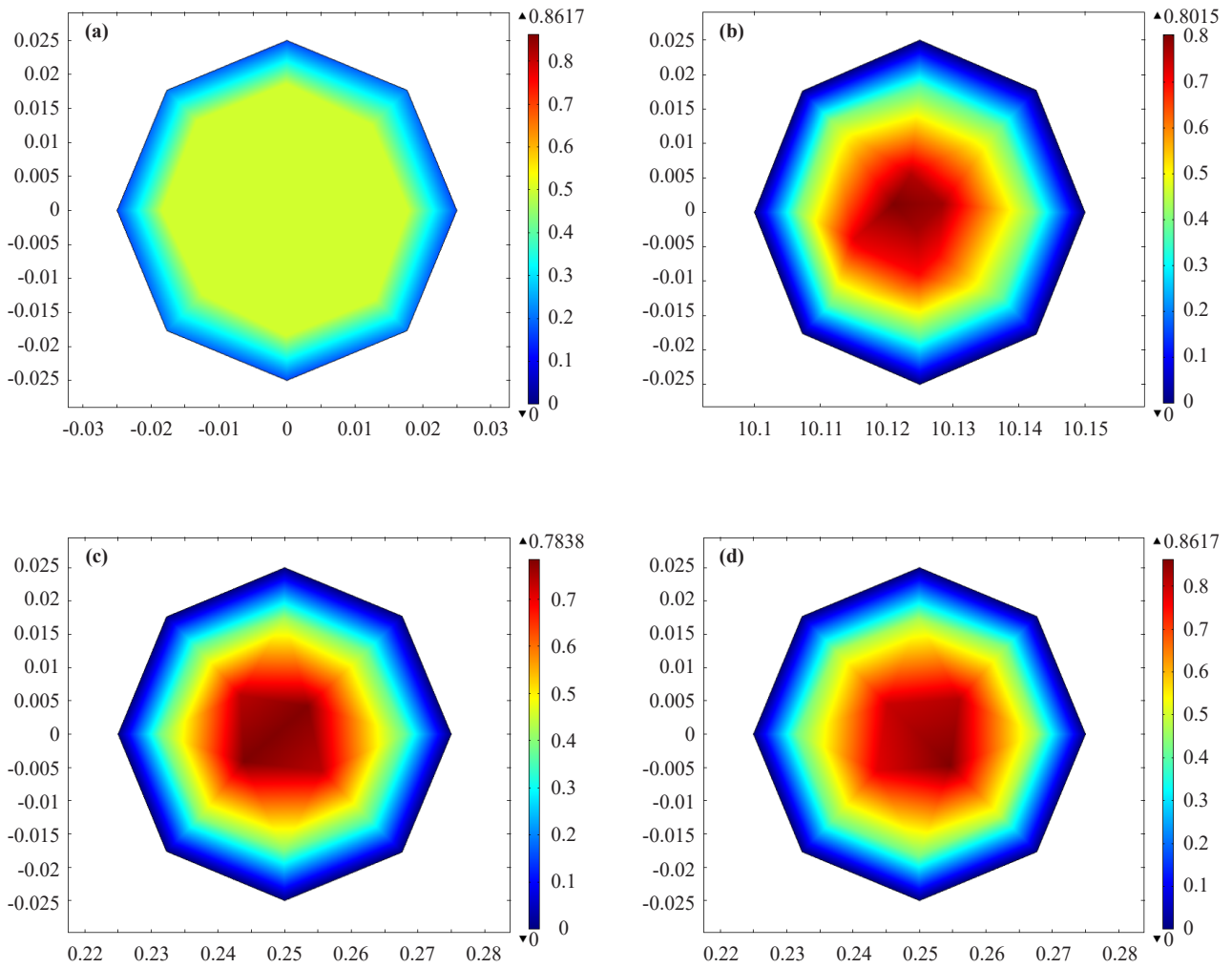


Figure 4. A longitudinal view of the velocity profiles on the horizontal cross-section ( $z = 0$ ) for a portion of the reactor geometry at 11:00 AM

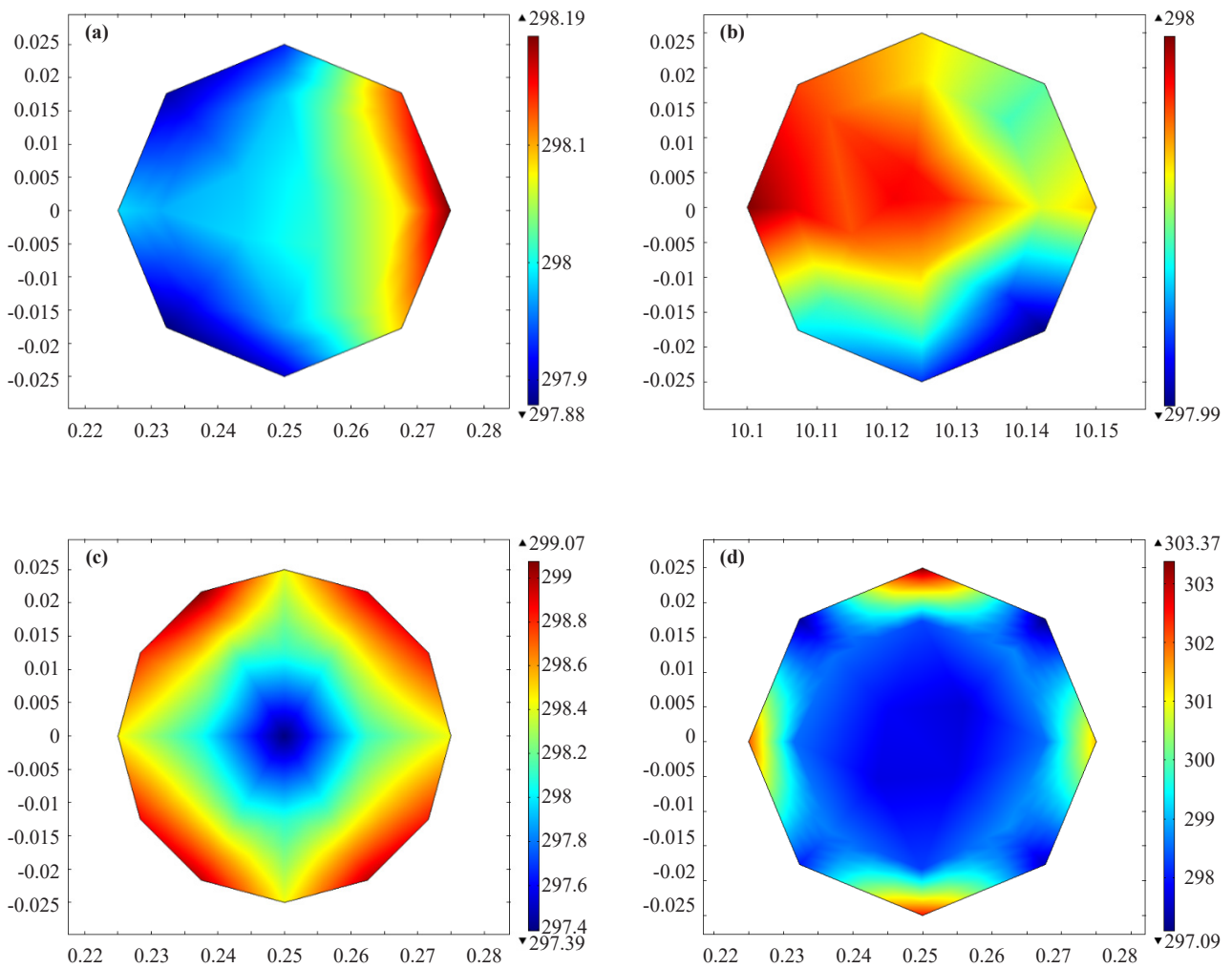
Figure 5(a) to Figure 5(d) shows the velocity profiles at different vertical cross-sections of the domain at 11:00 AM.



**Figure 5.** (a) Velocity profiles on the vertical cross-section at inlet at 11:00 AM; (b) Velocity profiles on the vertical cross-section at the middle of the U-loop at 11:00 AM; (c) Velocity profiles on the vertical cross-section at  $x = 10$  m (measured from outlet) at 11:00 AM; (d) Velocity profiles on the vertical cross-section at outlet at 11:00 AM

From the velocity profiles illustrated above, it is observed that at 11:00 AM, the velocity at the middle of the tube is same as the initial velocity at the inlet whereas it gradually tends to zero near the wall. In case of other cross-sections, the maximum velocity of around  $0.85 \text{ ms}^{-1}$  is found in the middle of the pipe while it approaches to zero as we reach near the reactor wall. This gives a parabolic shape of the flow. It is also noticed that the velocity is more or less symmetric with respect to a vertical line drawn at arc length  $0.025 \text{ m}$ . It is worth mentioning that when the culture flow crosses the U-loop, it is skewed towards the outer side of the tube wall. However, before crossing the U-loop it is skewed towards the inner part.

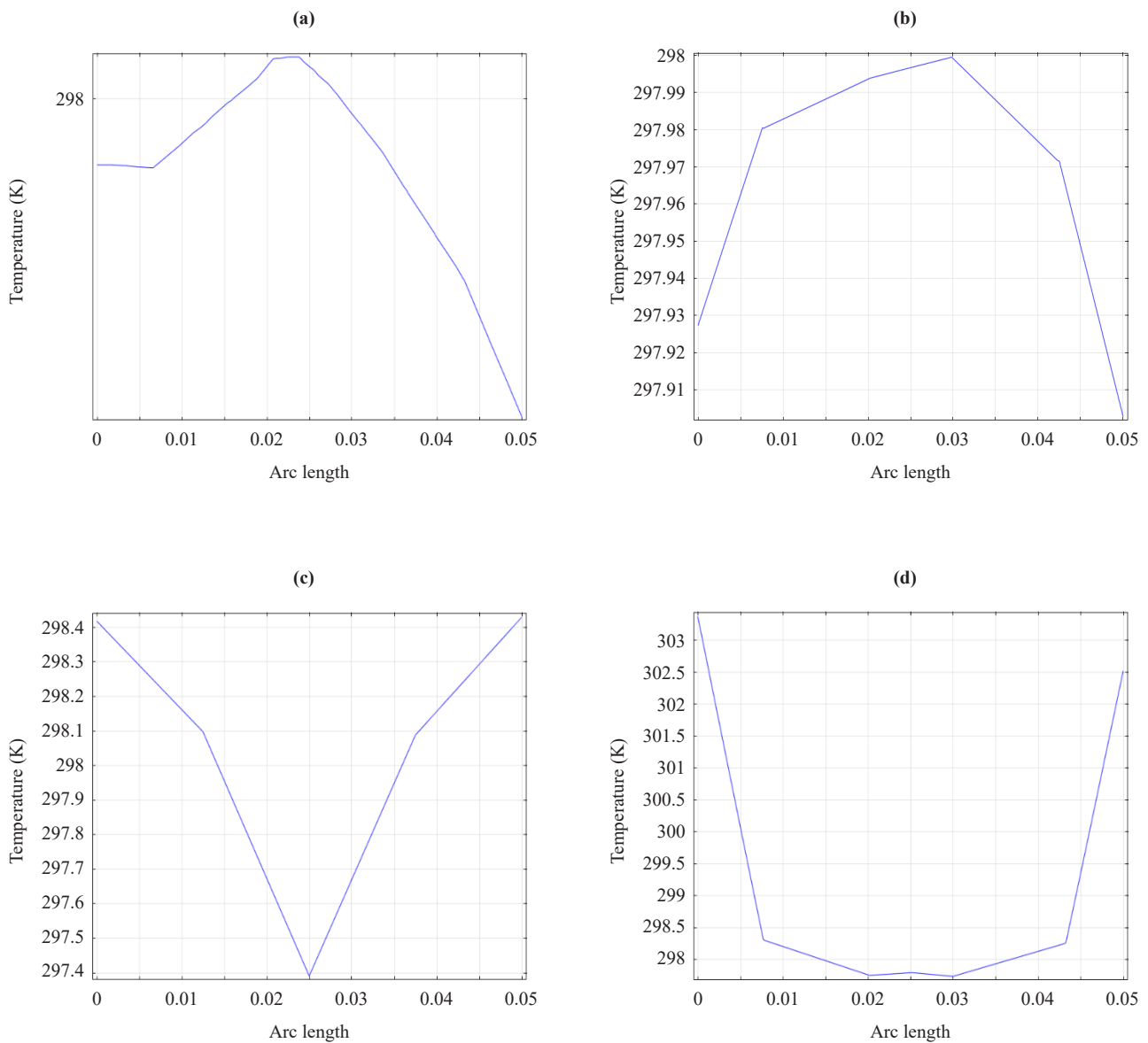
Figure 6(a) to Figure 6(d) shows the temperature profiles at different vertical cross-sections of the domain at 11:50 AM



**Figure 6.** (a) Temperature profiles on the vertical cross-section at the middle of U-loop at 11:50 AM; (b) Temperature profiles on the vertical cross-section at  $x = 10$  m (measured from outlet) at 11:50 AM; (c) Temperature profiles on the vertical cross section at  $x = 5$  m (measured from outlet) at 11:50 AM; (d) Temperature profiles on the vertical cross-section at outlet at 11:50 AM

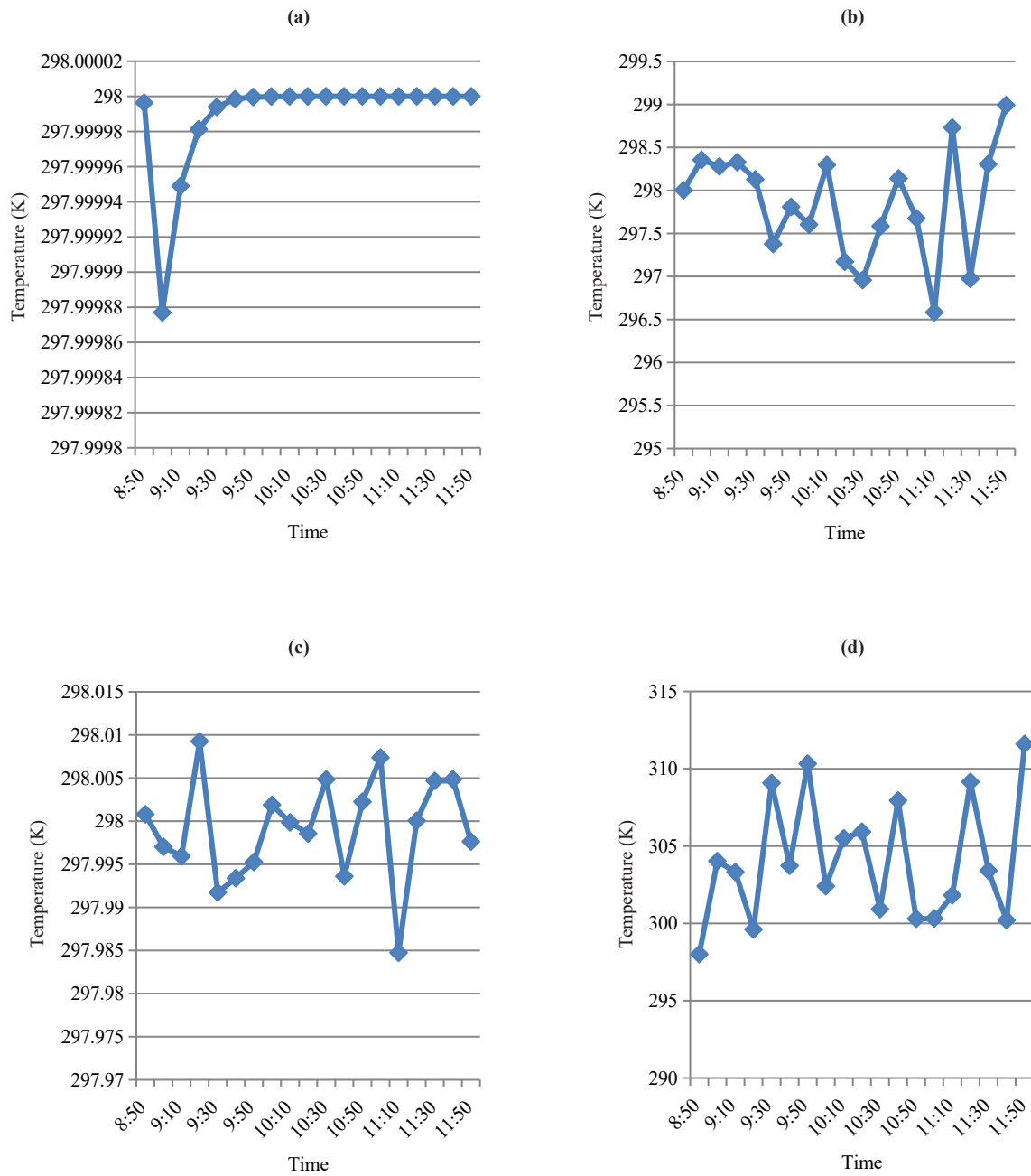
This means that viscosity of the flow was decreasing towards the outlet of the domain. On the other hand, Figure 7(a) to Figure 7(d) depicts the temperature magnitudes on the vertical diameters of those cross-sections for the same time.

From the temperature profiles (Figure 6 (a-d)) and magnitudes (Figure 7 (a-d)) illustrated above, it was observed that at 11:50 AM, the temperature remains almost constant at the cross-sections in the inlet side with small fluctuations in the middle of the U-loop. However, a significant variation of temperature was observed at different vertical cross-sections in the outlet side. It is interesting to note that at the cross-section 10 m away from the outlet, temperature is higher in the middle of the tube compared to that of the wall whereas the opposite behaviour is observed for the cross-sections 5 m apart from the outlet and at the outlet itself.



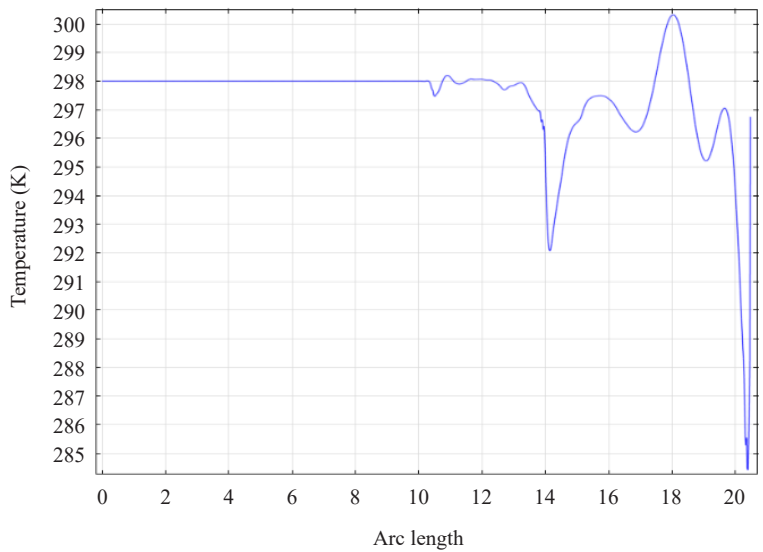
**Figure 7.** (a) Temperature magnitudes on the vertical diameter of the vertical cross-section at the middle of the U-loop at 11:50 AM; (b) Temperature magnitudes on the vertical diameter of the vertical cross-section at  $x = 10$  m (measured from outlet) at 11:50 AM; (c) Temperature magnitudes on the vertical diameter of the vertical cross-section at  $x = 5$  m (measured from outlet) at 11:50 AM; (d) Temperature magnitudes on the vertical diameter of the vertical cross-section at outlet at 11:50 AM

Figure 8(a) to Figure 8(c) illustrates the temperature variation with time for different vertical cross-sections of the domain. From these graphs, it was observed that for the cross-section 5 m away from the inlet, the temperature drops significantly at 9:00 AM and half an hour later it regains its previous figure which continues till the end of the simulation time. On the contrary, the temperature keeps fluctuating throughout the time period for the vertical cross-sections at the outlet and at the middle of the U-loop. Figure 8(d) depicts the temperature variation with time for the entire reactor domain. From the graph, it is noticed that the temperature fluctuates between 298 K and 311.6 K over the three-hour time period.



**Figure 8.** (a) Temperature variations with time at  $x = 5$  m (measured from inlet); Figure 8(a) Temperature variations with time at  $x = 5$  m (measured from inlet); (c) Temperature variations with time at the middle of the U-loop; (d) Variations of temperature with time for the entire domain

Figure 9 depicts the variations of temperature along the longitudinal arc length at time 11:00 AM. From the graph, it was noticed that the temperature remains the same for the arc length from the inlet to the U-loop, and it continues fluctuating till the outlet.



**Figure 9.** Temperature magnitudes along the longitudinal arc length at 11:00 AM

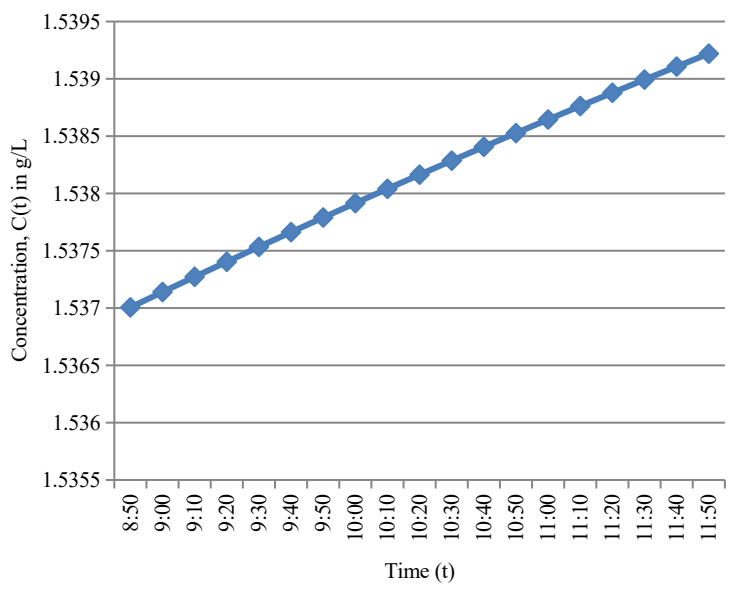


**Figure 10.** Change of microalgae cell concentration with respect to time at the vertical cross-section  $x = 5$  m

Figure 10 illustrates the change of microalgae cell concentration with respect to time for vertical cross-section at  $x = 5$  m from the inlet of the domain. From the graph, a very slow growth of concentration is noticed throughout the time that depict a growth response of culture cell from the present model.

Thus, it can strongly admit that temperature is one of the most essential ingredients for the growth of microalgae cell. Now it is clear that this parameter must be monitored more attentively and systematically along the cultures. Further research can verify the present existing model and may help to visualize the effective impacts of temperature on HLTP.

## 4. Conclusions

In this work, the variation of irradiance related temperature and its effect on the microalgae growth were analysed over specific time duration. The simulation had been carried out on the seventh day of the microalgae culture. The velocity profile of the suspension flow was observed at different cross-sections at different time and the velocity was found higher in the middle of the tube which decreased gradually towards the reactor wall forming a parabolic shape. Studying the temperature variation of the reactor at different cross-sections at different times, it is surprisingly seemed that for the straight portion from the inlet side, the variation is negligible during the simulated time range. However, it was changed erratically for the rest of the reactor domain. Maximum temperature was reported to be 311.6 K (38.45 °C) at 11:50 AM which is beyond the optimal temperature range (20 °C-35 °C). Thus, the present work is suggesting for using shades, spraying water or installing a heat exchanger in the PBR in order to maintain the suspension temperature in favourable condition. This study will increase the microalgae cell growth in HLTP which may play a great role in renewable biofuel research.

## Acknowledgement

The authors gratefully acknowledge for the technical supports provided by the Centre of Excellence in Mathematics, Department of Mathematics, Mahidol University, Bangkok-10400, Thailand and the Simulation Lab, Department of Mathematics, Chittagong University of Engineering and Technology, Chattogram-1349, Bangladesh.

## Conflict of interest

The authors declare no competing financial interest.

## References

- [1] Halder P, Paul N, Joardder M, Sarker M. Energy scarcity and potential of renewable energy in Bangladesh. *Renewable and Sustainable Energy Reviews*. 2015; 51: 1636-1649. Available from: <https://doi.org/10.1016/j.rser.2015.07.069>.
- [2] Mata TM, Martins AA, Caetano NS. Microalgae for biodiesel production and other applications: A review. *Renewable and Sustainable Energy Reviews*. 2010; 14: 217-232. Available from: <https://doi.org/10.1016/j.rser.2009.07.020>.
- [3] Yen HW, Hu IC, Chen CY, Nagarajan D, Chang JS. Design of photobioreactors for algal cultivation. In: Pandey A, Chang JS, Soccol CR, Lee DJ. (eds.) *Biofuels from Algae*. 2nd ed. Elsevier; 2019. p.225-256. Available from: <https://doi.org/10.1016/B978-0-444-64192-2.00010-X>.
- [4] Sergio M, Natalia D, Yogi H. Algae communication, conspecific and interspecific: The concepts of phycosphere and algal-bacteria consortia in a photobioreactor (PBR). *Plant Signaling & Behavior*. 2023; 18(1): 2148371. Available from: <https://doi.org/10.1080/15592324.2022.2148371>.
- [5] Ación Fernández FG, Fernández Sevilla JM, Molina Grima E. Photobioreactors for the production of microalgae. *Reviews in Environmental Science and Bio/Technology*. 2013; 12(2): 131-151. Available from: <https://doi.org/10.1007/s11157-012-9307-6>.
- [6] Posten C. Design principles of photo-bioreactors for cultivation of microalgae. *Engineering in Life Sciences*. 2009; 9(3): 165-177. Available from: <https://doi.org/10.1002/elsc.200900003>.
- [7] Ras M, Steyer J, Bernard O. Temperature effect on microalgae: A crucial factor for outdoor production. *Reviews in Environmental Science and Bio/Technology*. 2013; 12(2): 153-164. Available from: <https://doi.org/10.1007/s11157-013-9310-6>.
- [8] Chowdury K, Nahar N, Deb UK. The growth factors involved in microalgae cultivation for biofuel production: A review. *Computational Water, Energy, and Environmental Engineering*. 2020; 9(4): 185-215. Available from: <https://doi.org/10.4236/cweee.2020.94012>.
- [9] Bernard O, Rémond B. Validation of a simple model accounting for light and temperature effect on

microalgal growth. *Bioresource Technology*. 2012; 123: 520-527. Available from: <https://doi.org/10.1016/j.biortech.2012.07.022>.

- [10] Tobias W, Claudia G, Micheal P. Experimental and model-based analysis to optimize microalgal biomass productivity in a pilot-scale tubular photobioreactor. *Frontiers in Bioengineering and Biotechnology*. 2020; 8: 453. Available from: <https://doi.org/10.3389/fbioe.2020.00453>.
- [11] Huesemann M, Van WJ, Miller T, Chavis A, Hobbs S, Crowe B. A screening model to predict microalgae biomass growth in photobioreactors and raceway ponds. *Biotechnology and Bioengineering*. 2013; 110(6): 1583-1594. Available from: <https://doi.org/10.1002/bit.24814>.
- [12] Goncalves AL, Pires LCM, Simões M. The effects of light and temperature on microalgal growth and nutrient removal: An experimental and mathematical approach. *RSC Advances*. 2016; 6(27): 22896-22907. Available from: <https://doi.org/10.1039/C5RA26117A>.
- [13] Govindarajan RK, Thiruvengadam R, Alanazi AA, Pandiaraj S, Mathivanan K, Thiruvengadam M, et al. Optimization of photosynthetically active radiation, temperature, and urea deprivation for increasing neutral lipids and fatty acids in *Scenedesmus obliquus* and *Chlorella vulgaris* as biodiesels. *Biomass and Bioenergy*. 2023; 174: 106854. Available from: <https://doi.org/10.1016/j.biombioe.2023.106854>.
- [14] Ras M, Steyer JP, Bernard O. Temperature effect on microalgae: A crucial factor for outdoor production. *Reviews in Environmental Science and Bio/Technology*. 2013; 12(2): 153-164. Available from: <https://doi.org/10.1007/s11157-013-9310-6>.
- [15] Sheekh ME, Fatah EA, Azim AM, Shanab AR. Effect of temperature on growth and fatty acids profile of the biodiesel producing microalga *Scenedesmus acutus*. *Biotechnologie, Agronomie, Société et Environnement/ Biotechnology, Agronomy, Society and Environment*. 2017; 21(4): 233-239. Available from: <https://doi.org/10.25518/1780-4507.15291>.
- [16] Kathirvel B, Thangavel M, Eldon RR, Sabarathinam S, Nguyen TLC, Arivalagan P. Impact of cultivation conditions on the biomass and lipid in microalgae with an emphasis on biodiesel. *Fuel*. 2021; 284: 119058. Available from: <https://doi.org/10.1016/j.fuel.2020.119058>.
- [17] Deb UK, Chayantrakom K, Lenbury Y. Comparison of single-phase and two-phase flow dynamics in the HLTP for microalgae culture. *International Journal of Mathematics and Computers in Simulation*. 2012; 6: 496-503.
- [18] Singh SP, Priyanka S. Effect of temperature and light on the growth of algae species: A review. *Renewable and Sustainable Energy Reviews*. 2015; 50: 431-444.
- [19] Zhou H, Li X, Xu G, Yu H. Overview of strategies for enhanced treatment of municipal/domestic wastewater at low temperature. *Science of the Total Environment*. 2018; 643: 225-237.
- [20] Gaignar C, George Z, Buso Z. Influence of different abiotic factors on lipid production by microalgae-A review. *Oilseeds and Fats, Crops and Lipids*. 2021; 28: 57. Available from: <https://doi.org/10.1051/ocl/2021045>.
- [21] Xueying M, Shanshan G, Yang L, Jie H, Vladimir R, Lars GR, et al. Effects of elevated temperature on resources competition of nutrient and light between benthic and planktonic algae. *Frontiers in Environmental Science*. 2022; 10: 908088. Available from: <https://doi.org/10.3389/fenvs.2022.908088>.
- [22] Yin Z, Zhu L, Li S, Hu T, Chu R, Mo F, et al. A comprehensive review on cultivation and harvesting of microalgae for biodiesel production: Environmental pollution control and future directions. *Bioresource Technology*. 2020; 301: 122804.
- [23] Bitog JP, Lee IB, Lee CG, Kim KS, Hwang HS, Hong SW, et al. Application of computational fluid dynamics for modeling and designing photobioreactors for microalgae production: A review. *Computers and Electronics in Agriculture*. 2011; 76(2): 131-147. Available from: <https://doi.org/10.1016/j.compag.2011.01.015>.
- [24] Shahriar M, Deb UK, Rahman KA. Simulation of temperature effect on microalgae culture in a tubular photo bioreactor for local solar irradiance. *AIP Conference Proceedings*. 2017; 1851: 020021. Available from: <https://doi.org/10.1063/1.4984650>.
- [25] Deb UK, Shahriar M, Bhowmik J, Chowdury M. The effect of irradiance related temperature on microalgae growth in a tubular photo bioreactor for cleaner energy. *American Journal of Computational Mathematics*. 2017; 7(3): 371-384. Available from: <https://doi.org/10.4236/ajcm.2017.73026>.
- [26] Einstein A. A new determination of molecular dimensions. *Annalen der Physik*. 1906; 19: 289-306. Available from: <https://nfn.mit.edu/sites/default/files/documents/sr-2007-1.pdf>.
- [27] Hon-nami K, Kunito S. Microalgae cultivation in a tubular bioreactor and utilization of their cells. *Chinese Journal of Oceanology and Limnology*. 1998; 16(S1): 75-83. Available from: <https://doi.org/10.1007/bf02849084>.
- [28] Androga D, Uyar B, Koku H, Eroglu I. Dynamic modeling of temperature change in outdoor operated tubular photobioreactors. *Bioprocess and Biosystems Engineering*. 2017; 40(7): 1017-1031. Available from: <https://doi.org/10.1007/s00449-017-1765-3>.



- [29] Bechet Q, Shilton A, Fringer OB, Munoz R, Guieysse B. Mechanistic modeling of broth temperature in outdoor photobioreactors. *Environmental Science & Technology*. 2010; 44: 2197-2203. Available from: <https://doi.org/10.1021/ES903214U>.
- [30] Duffie JA, Beckman WA. *Solar Engineering of Thermal Process*. New Jersey, USA:Wiley; 2006.
- [31] Camacho FG, Gomez AC, Fernandez FGA, Sevilla JF, Grima EM. Use of concentric-tube airlift photobioreactors for microalgal outdoor mass cultures-Mixing, carbon utilization, and oxygen accumulation. *Enzyme and Microbial Technology*. 1999; 24: 164-172. Available from: [https://doi.org/10.1016/S0141-0229\(98\)00103-3](https://doi.org/10.1016/S0141-0229(98)00103-3).
- [32] Almorox JY, Hontoria CJEC. Global solar radiation estimation using sunshine duration in Spain. *Energy Conversion and Management*. 2004; 45(9-10): 1529-1535. Available from: <https://doi.org/10.1016/j.enconman.2003.08.022>.
- [33] Sarkar MNI. Estimation of solar radiation from cloud cover data of bangladesh. *Renewables: Wind, Water and Solar*. 2016; 3(11): 1-15. Available from: <https://doi.org/10.1186/s40807-016-0031-7>.
- [34] Mehlitz TH. *Temperature influence and heat management requirements of microalgae cultivation in photobioreactors*. California Polytechnic State University; 2009. Available from: <https://doi.org/10.15368/theses.2009.15>.